The insulin-like growth factor-I (IGF-I) receptor kinase inhibitor NVP-ADW742, in combination with STI571, delineates a spectrum of dependence of small cell lung cancer on IGF-I and stem cell factor signaling

G. Sakuntala Warshamana-Greene,[1] Julie Litz,[1] Elisabeth Buchdunger,[2] Francesco Hofmann,[2] Carlos García-Echeverría,[2] and Geoffrey W. Krystal[1]

[1]Department of Medicine, Virginia Commonwealth University and McGuire Veterans Affairs Medical Center, Richmond, Virginia and [2]Novartis Institutes for BioMedical Research, Novartis Pharma AG, Basel, Switzerland

Abstract

Stem cell factor (SCF)/Kit and insulin-like growth factor-I (IGF-I)/IGF-I receptor (IGF-IR) autocrine loops play a prominent role in the growth of small cell lung cancer (SCLC). Previous data suggested that IGF-I protects cells from apoptosis induced by STI571, an efficient inhibitor of Kit signal transduction, by activating the critical phosphatidylinositol 3-kinase-Akt pathway. To determine if inhibition of IGF-IR signaling would be therapeutically relevant in SCLC, the activity of a novel kinase inhibitor of IGF-IR, NVP-ADW742 (Novartis Pharma AG, Basel, Switzerland), was characterized. Pretreatment of the H526 cell line with NVP-ADW742 inhibited IGF-IR signaling and growth with IC_{50} values between 0.1 and 0.4 μM. SCF-mediated Kit phosphorylation and Akt activation were inhibited with IC_{50} values in the 1–5 μM range. However, NVP-ADW742 affected neither hepatocyte growth factor-mediated Akt activation nor activity of constitutively active Akt. The therapeutic potential of NVP-ADW742 was assessed by determining its effect on growth of several SCLC cell lines in serum. These studies clearly delineated two populations of cell lines as determined by differential sensitivity to NVP-ADW742. One population, which lacks active SCF/Kit autocrine loops, was inhibited with IC_{50} values between 0.1 and 0.5 μM. A second population, which has active SCF/Kit autocrine loops, was inhibited with IC_{50} values in the 4–7 μM range. When these cell lines were treated with a combination of STI571 and NVP-ADW742, no advantage was seen in the former group, whereas, in the latter group, a clearly synergistic response to the combination was seen when growth, apoptosis, or Akt activation was assessed. These data demonstrate that NVP-ADW742 is a potent and selective IGF-IR kinase inhibitor that can efficiently inhibit the growth of cells that are highly dependent on IGF-I signaling. However, for optimal growth inhibition of SCLC cells with an active SCF/Kit autocrine loop, a combination of a Kit inhibitor (STI571) and an IGF-IR inhibitor (NVP-ADW742) appears to be necessary. These observations suggest that, in tumors in which critical signal transduction pathways can be activated by alternative receptors, optimal therapy may require inhibition of multiple receptors. [Mol Cancer Ther 2004;3(5):527–35]

Introduction

Insulin-like growth factor-I (IGF-I) is a peptide hormone critical for growth, development, and oncogenic transformation (1–4). Its effects are exerted through the IGF-I receptor (IGF-IR), a member of the insulin receptor subclass of receptor tyrosine kinases. Mice null for either IGF-I or its receptor are born markedly underweight. *IGF-I−/−* mice reach only 30% of normal adult body weight, exhibit delayed bone development, and are infertile. Homozygous knockout of the *IGF-IR* results in perinatal lethality (5, 6). IGF-I is a potent mitogen for a wide variety of cells, promoting cell cycle progression by stimulating the expression of cyclin D1 (7). It is also a potent regulator of cellular survival and apoptosis predominantly by activating the phosphatidylinositol 3-kinase (PI3K)-Akt intracellular signaling pathway and its divergent downstream signaling cascades (8). IGF-I has been shown to directly stimulate the expression of Bcl-2 and Bcl-X_L and suppress the expression of Bax, resulting in inhibition of apoptosis (9, 10).

Based on its combined effects on mitogenic and antiapoptotic signaling, IGF-I has been implicated in the establishment and maintenance of the transformed phenotype in many cellular backgrounds (11, 12). Murine fibroblasts with a targeted disruption of the *IGF-IR* gene are refractory to transformation by a wide variety of potent oncogenes that readily transform wild-type fibroblasts (3, 4). Epidemiological studies have shown that increased serum levels of IGF-I and decreased levels of its predominant binding protein, IGFBP-3, correlate with an increased risk for several types of cancers (13, 14). For example, high plasma levels of IGF-I are associated with a 2.75-fold increased risk of lung cancer while high plasma levels of IGFBP-3 are associated with a reduced risk compared with control subjects (15).

Received 12/12/03; revised 1/30/04; accepted 3/2/04.

Grant support: Supported in part by a Merit Review Award from the Department of Veterans Affairs (G.W. Krystal).

The costs of publication of this article were defrayed in part by the payment of page charges. This article must therefore be hereby marked advertisement in accordance with 18 U.S.C. Section 1734 solely to indicate this fact.

Requests for Reprints: Geoffrey W. Krystal, Richmond Veterans Affairs Medical Center (111K), 1201 Broad Rock Boulevard, Richmond, VA 23249. Phone: (804) 675-5446; Fax: (804) 675-5447. E-mail: gkrystal@hsc.vcu.edu

Small cell lung cancer (SCLC) represents 20–25% of newly diagnosed cases of lung cancer and, despite high initial response rates to chemotherapy, causes the demise of 90–95% of affected individuals (16). IGF-I is an important growth factor for SCLC cells in both endocrine and autocrine contexts (17–19). IGF-I is a very potent stimulator of PI3K-Akt signaling in SCLC in terms of both the degree of activation and the length of time the pathway remains activated after stimulation (20). Growth stimulated by IGF-I is largely mediated by PI3K-Akt signaling, which also enhances resistance to the apoptotic effect of chemotherapy (20). Given the above, inhibition of IGF-I signaling could be an important novel therapeutic approach in SCLC. However, other receptor tyrosine kinases, such as Kit, the stem cell factor (SCF) receptor, also stimulate SCLC growth via the PI3K-Akt pathway (20). Treatment of SCLC cells with STI571 (imatinib mesylate; Gleevec/Glivec), a highly efficient small molecule Kit inhibitor (21–23), retards growth of SCLC cell lines but fails to induce apoptosis if IGF-I is present in the medium, either alone or as a component in serum (22). Given these observations, the potential therapeutic benefit of selective IGF-IR inhibition is unclear.

We therefore chose to investigate the effects of a novel selective small molecule IGF-IR kinase inhibitor NVP-ADW742 (24, 25) on the growth of SCLC cells, alone and in combination with STI571. NVP-ADW742 is a pyrrolo [2,3-*d*]pyrimidine derivative that binds in the ATP binding pocket of the IGF-IR and inhibits its *in vitro* kinase activity with an IC_{50} of 0.1–0.2 μM (24, 25). While the IC_{50} of the insulin receptor is similar in *in vitro* assays using the recombinant kinase domain of this receptor, the cellular IC_{50} for inhibition of insulin receptor autophosphorylation is 15-fold greater (2.8 μM) than that of the IGF-IR (IC_{50} of 0.17 μM). The selectivity observed at the cellular level suggests that, despite the high degree of identity of the kinase domains of the IGF-I and insulin receptors, there are conformational differences between the native forms of these receptors that are not recapitulated by the respective recombinant kinase domains used in the biochemical assays. The *in vitro* IC_{50} values for a broad panel of tyrosine and serine/threonine kinases, including c-Abl, epidermal growth factor receptor, Her-2, platelet-derived growth factor receptor, vascular endothelial growth factor receptor-2, Flt-4, fibroblast growth factor receptor-1, c-Met, Raf-1, protein kinase A, c-Src, cyclin-dependent kinase 1, protein kinase B, and phosphoinositide-dependent kinase 1, were all at least 10-fold higher than the recombinant IGF-IR kinase domain. Cellular assays revealed IC_{50} values greater than 10 μM for epidermal growth factor receptor, platelet-derived growth factor receptor, and vascular endothelial growth factor receptor-2. The compound did show potent inhibition of Flt-3 (IC_{50} of 0.068 μM), Flt-1 (IC_{50} of 0.57 μM), and Tek (IC_{50} of 0.41 μM) recombinant kinase domains (24, 25). However, there is no published evidence for expression of the latter receptor tyrosine kinases in SCLC, and stimulation with ligands for Flt-1 and Flt-3 did not induce signal transduction or growth when a panel of SCLC cell lines was tested (J. Litz and G. W. Krystal, unpublished observations).

To initially document specificity in SCLC cell lines, we studied the relative effects of NVP-ADW742 on IGF-I- and SCF-mediated signaling. NVP-ADW742 inhibited IGF-I-mediated signaling and growth with IC_{50} values in the submicromolar range, while values for SCF were ~10-fold higher. Two populations of SCLC cell lines were identified based on their response to NVP-ADW742 in complete medium. Growth of cell lines that lack an active SCF/Kit autocrine loop was inhibited with IC_{50} values between 0.1 and 0.5 μM, whereas growth of cell lines that have an active SCF/Kit autocrine loop was inhibited with IC_{50} values at least 10-fold higher. In growth assays where cells were treated with a combination of STI571 and NVP-ADW742, no advantage was seen in the former group, whereas, in the latter group, a clearly synergistic response to the combination was observed. This synergistic growth inhibition correlated with synergistic inhibition of PI3K-Akt activity. These data demonstrate that the selective IGF-IR inhibitor NVP-ADW742 potently blocks growth of cells that are highly dependent on IGF-I signaling. However, for cells that have an active SCF/Kit autocrine loop, blocking both Kit and IGF-IR kinase activity is necessary for optimal growth inhibition. Importantly, this observation suggests that for tumors that rely on alternative receptors for activation of critical signaling pathways, therapeutic strategies designed to block signaling from multiple receptors may have to be developed.

Materials and Methods

Compounds

STI571 and NVP-ADW742 were synthesized and provided by Novartis Pharma AG (Basel, Switzerland). Stock solutions were made in 100% DMSO (Sigma Chemical Co., St. Louis, MO) and diluted with culture media before use. The final DMSO concentration in all cultures, including vehicle controls, was 0.1%.

Cell Growth

All previously characterized SCLC cell lines (26, 27) were cultured in complete medium, which consisted of 10% (v/v) fetal bovine serum (FBS; Invitrogen Life Technologies, Inc., Carlsbad, CA), 2 mM L-glutamine (Bio Whittaker, Walkersville, MD), and 50 units/ml penicillin-streptomycin (Bio Whittaker) in RPMI 1640 (Invitrogen Life Technologies). When FBS was omitted, 0.1% BSA (Sigma Chemical) was added to the medium. Where indicated, the serum-free medium was supplemented with 10 ng/ml IGF-I (R&D Systems, Inc., Minneapolis, MN), 100 ng/ml SCF (Peprotech, Rocky Hill, NJ), or 100 ng/ml hepatocyte growth factor (HGF; R&D Systems). MRC-5 pulmonary fibroblasts and NIH3T3 cells were purchased from American Type Culture Collection (Manassas, VA) and maintained in Eagle's MEM (Invitrogen Life Technologies) supplemented with 10% FBS, 2 mM L-glutamine, and 50 units/ml penicillin-streptomycin. Primary normal human bronchial epithelial cells were maintained in the medium provided by the supplier (Clonetics Bio Whittaker). FBS (10%) was added to the basal medium when the cells were incubated in NVP-ADW742. R-cells were kindly

donated by Dr. Renato Baserga and maintained in DMEM (Invitrogen Life Technologies) supplemented with 10% FBS, 2 mM L-glutamine, and 50 units/ml penicillin-streptomycin. Cell growth was measured using the 3-(4,5-dimethylthiazol-2-yl)-2,5-diphenyltetrazolium bromide (MTT; Sigma Chemical) colorimetric dye reduction method, an assay shown to correlate very well with viable SCLC cell number under the conditions used (28). Duplicate plates containing eight replicate wells per assay condition were seeded at a density of 1×10^4 cells in 0.1 ml of medium and relative growth was determined by the change in absorbance at 540 nm over 72 h relative to initial values obtained 3 h after plating. For each experiment, a dose-response curve was generated by plotting percentage change in growth relative to control treatment against inhibitor concentration. For assessment of efficiency of growth inhibition, an IC_{50} value was calculated using the dose-response curve. Results from drug combination studies were analyzed with the multiple drug effect equation (29) using Calcusyn software (Biosoft, Ferguson, MO).

Preparation of Cell Lysates, Immunoprecipitation, and Western Analysis

Cells quiesced overnight in serum-free medium were pretreated with either DMSO or the inhibitor (NVP-ADW742 or STI571) for 1 h at 37°C. Subsequently, the cells were either left unstimulated or stimulated with 10 ng/ml IGF-I, 100 ng/ml SCF, or 100 ng/ml HGF for 15 min. The stimulation was stopped with the addition of cold PBS, and cells were pelleted and resuspended in cold PBS. To prepare whole cell lysates, an equal volume of 2× SDS sample buffer [2% SDS, 0.08 M Tris-HCl (pH 6.8), 10% glycerol] was added and the cell suspension was sheared through a 25 gauge needle. Protein concentrations were determined (BCA; Pierce Chemical Co., Rockford, IL) and 50 μg of protein were resolved on a 10% polyacrylamide gel. For immunoprecipitation, cells were pelleted and resuspended in single detergent lysis buffer described previously (20). Lysate (1 mg) was used for immunoprecipitation with either 10 μg polyclonal anti-IGF-IRα antibody (Cell Signaling Technology, Beverly, MA), 3 μg polyclonal anti-IGF-IRβ antibody (Santa Cruz Biotechnology, Santa Cruz, CA), or 10 μg affinity-purified anti-c-Kit antibody raised against amino acids 961–976 of c-Kit. The immunoprecipitated samples were resuspended in SDS loading buffer and resolved on a 10% polyacrylamide gel.

Standard procedures were used in carrying out Western blotting and bands were visualized using the enhanced chemiluminescence system (Amersham, Arlington Heights, IL) with the aid of a Fuji (Tokyo, Japan) cooled CCD camera. The Aida 2.0 software package (Raytest, Inc., New Castle, DE) was used to quantitate the band intensity. For determination of relative kinase activity, the intensity of the band representing the phosphorylated form of the kinase was normalized against the band representing total kinase. For assessment of inhibition of phosphorylation by a given inhibitor, a response curve was generated by plotting percentage change in kinase activity against inhibitor concentration and an IC_{50} value was calculated using the response curve.

The following antibodies were used in immunoblotting: anti-phosphotyrosine (anti-pTyr) PY20 and PY99 monoclonal, anti-pan-Akt polyclonal, and anti-pan-glycogen synthase kinase (GSK)-3β monoclonal (Santa Cruz Biotechnology); anti-IGF-IRα, anti-phospho-Kit (Tyr^{721}) [pKit (Tyr^{721})], anti-phospho-Akt (Ser^{473}) [pAkt (Ser^{473})], anti-phospho-44/42-mitogen-activated protein kinase (MAPK), and anti-phospho-GSK-3α/β polyclonal (Cell Signaling Technology); anti-pan-MAPK polyclonal (Upstate Biotechnology, Inc., Lake Placid, NY); and anti-Kit polyclonal (DAKO Corp., Carpinteria, CA).

Terminal Deoxynucleotidyltransferase-Mediated Nick End Labeling Assay

WBA cells were treated with NVP-ADW742 alone or NVP-ADW742 and STI571 for 24 h. Cell Tracker Orange (5 μM; Molecular Probes, Eugene, OR) was added to the cells and incubated for 30 min to readily allow identification of individual cells with fluorescence optics, and cytospin cell preparations were made. The cells were fixed and permeabilized and free DNA 3′ ends were labeled with fluorescein-conjugated dUTP mediated by terminal deoxynucleotidyltransferase (TdT) using the *In Situ* Cell Death Detection Kit (Roche Diagnostics, Mannheim, Germany) according to the manufacturer's instructions. Independent 600× fields containing a total of at least 500 cells were evaluated for nuclear labeling by fluorescence microscopy for each treatment. Cells treated with 25 μM etoposide (Calbiochem-Novabiochem, La Jolla, CA) were used as a positive control. Data were analyzed for significance using a Student's two-tailed *t* test.

Results

NVP-ADW742 Inhibits IGF-I-Mediated Receptor Activation

To determine the effect of NVP-ADW742 on IGF-IR activation, quiescent H526 cells were treated with either increasing concentrations of the drug or vehicle alone for 1 h followed by treatment with IGF-I for 15 min. A portion of the treated cells was used to prepare single detergent lysates at the end of the treatment period. IGF-IR in the lysate samples was immunoprecipitated and subjected to Western blotting using an anti-pTyr antibody to visualize the degree of IGF-I-stimulated tyrosine phosphorylation (Fig. 1). Cellular phosphorylation was inhibited by NVP-ADW742 with a mean IC_{50} of 0.1 μM (range of 0.05–0.2 μM; $n = 3$). Another portion of the treated cells was used to prepare whole cell lysates, which were used in a Western analysis to monitor PI3K-Akt pathway activation. IGF-I-mediated Akt activation was inhibited with a mean IC_{50} of 0.4 μM (range of 0.2–0.5 μM; $n = 3$; Fig. 1). The relatively modest level of MAPK activation produced by IGF-I in this cell line was inhibited with a similar IC_{50} (Fig. 1). These data suggest that NVP-ADW742 exhibits potent IGF-IR kinase inhibition at submicromolar doses.

To initially assess the specificity of the response, inhibition of SCF-mediated Kit tyrosine phosphorylation was measured in a similar experiment where the Kit receptor was immunoprecipitated with an anti-c-Kit

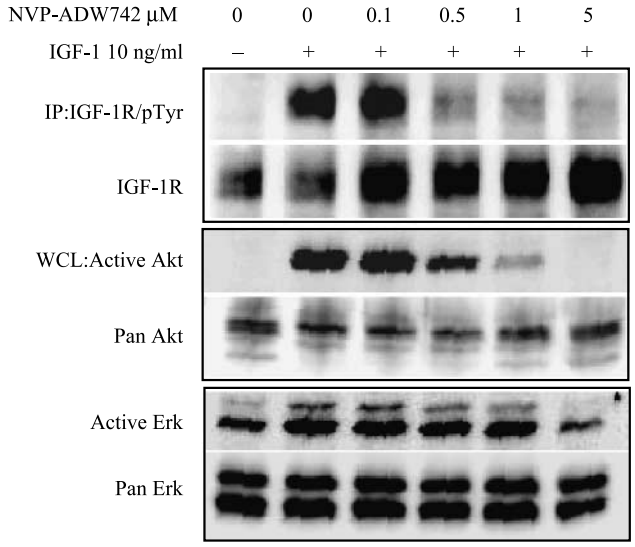

Figure 1. NVP-ADW742 inhibits IGF-I-mediated receptor activation. Lysates from quiescent H526 cells treated with either NVP-ADW742 or DMSO for 1 h followed by treatment with 10 ng/ml IGF-I for 15 min were analyzed by Western analysis. IGF-IR was immunoprecipitated from a portion of the treated cells and blotted with an anti-pTyr antibody to visualize the degree of IGF-I-stimulated tyrosine phosphorylation (*top panel*). Whole cell lysates from another portion of the treated cells were used to monitor the pAkt (Ser^{473}) and active Erk levels (*middle* and *lower panels*, respectively). Representative of three independent experiments.

antibody from NVP-ADW742- and SCF-treated H526 cell lysates. NVP-ADW742 inhibited Kit tyrosine phosphorylation with a mean IC_{50} of 2.2 μM (range of 1.9–2.7 μM; $n = 3$). When whole cell lysates from the same treated cell population were immunoblotted, Kit phosphorylation detected with an anti-pKit (Tyr^{721}) antibody was inhibited with a mean IC_{50} of 4.5 μM (range of 2.5–5.9 μM; $n = 4$). In the same lysates, Akt activation was inhibited with a mean IC_{50} of 1.6 μM (range of 1.2–2.6 μM; Fig. 2A). These data demonstrate that while Kit signaling is affected by NVP-ADW742, IGF-I signaling is ~10-fold more sensitive to the effects of the drug than is Kit signaling. Disparity between the results obtained for the Kit IC_{50} using the two different antibody techniques could be due to background detection of total Kit by the anti-pKit (Tyr^{721}) antibody as evidenced by significant staining of Kit in unstimulated cells using the anti-pKit (Tyr^{721}) antibody but not the anti-pTyr antibody (Fig. 2A).

Because SCF-mediated Akt activation appeared slightly more sensitive to NVP-ADW742 than was Kit phosphorylation, we felt it necessary to show that NVP-ADW742 is not a direct inhibitor of Akt activation. To determine whether Akt activation by another receptor tyrosine kinase would be affected, HGF-mediated Akt activation was assessed in the WBA SCLC cell line that expresses high levels of Met, the HGF receptor. Quiescent cells were treated with NVP-ADW742 followed by HGF and whole cell lysates were subjected to Western blotting. No inhibition of Akt phosphorylation was observed (Fig. 2B),

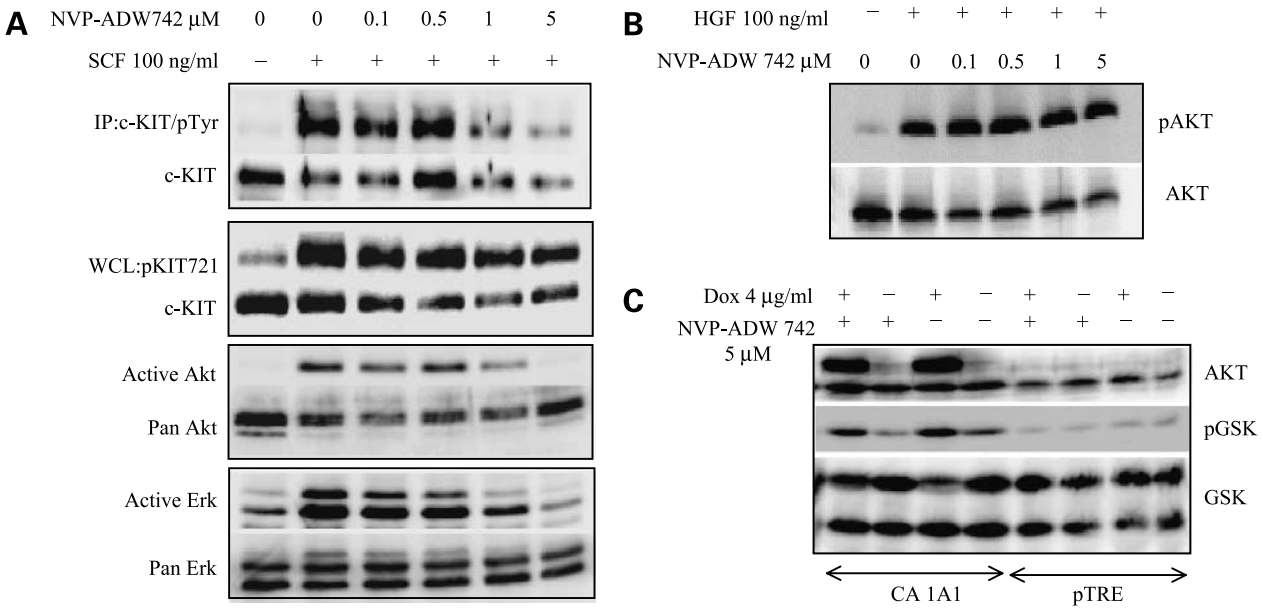

Figure 2. NVP-ADW742 inhibits SCF-mediated activation of Kit and Akt but is not a direct Akt inhibitor. **A,** lysates from quiescent H526 cells treated with either NVP-ADW742 or DMSO for 1 h followed by treatment with 100 ng/ml SCF for 15 min were analyzed by Western analysis. Kit was immunoprecipitated from a portion of the treated cells and blotted using an anti-pTyr antibody to visualize the degree of SCF-stimulated tyrosine phosphorylation (*top panel*). Whole cell lysates of the treated cells were used to monitor the pKit (Tyr^{721}), pAkt (Ser^{473}), and active Erk levels. Representative of four independent experiments. **B,** quiescent WBA cells were treated with NVP-ADW742 followed by 100 ng/ml HGF and whole cell lysates were subjected to Western blotting. No inhibition of Akt phosphorylation (Ser^{473}) was observed, indicating that treatment with NVP-ADW742, at the concentrations tested, did not affect HGF receptor-initiated activation of the PI3K-Akt pathway. **C,** whole cell lysates were prepared from CA 1A1 cells treated with either DMSO or 5 μM NVP-ADW742 in the presence or absence of doxycycline (*Dox*). Addition of the drug did not alter the level of GSK-3 phosphorylation induced by the expression of constitutively activated myristolated Akt. *pTRE,* vector control.

indicating that PI3K-Akt activation via Met is not affected by the compound. The lack of a direct effect on Akt activity was also confirmed by monitoring GSK-3 phosphorylation in CA 1A1 cells, which are H526 cells modified to express constitutively active myristolated Akt in a doxycycline-dependent fashion (20). Figure 2C shows that addition of NVP-ADW742 did not alter the levels of GSK-3 phosphorylation induced by expression of myristolated Akt. These results confirm that while Akt activation by both IGF-IR and Kit is affected by NVP-ADW742, the drug is not a direct Akt inhibitor. This is consistent with the lack of activity observed for this compound against Akt-1 in biochemical assays (IC_{50} > 10 μM, 0–10% inhibition at 10 μM; Ref. 25).

NVP-ADW742 Selectively Inhibits IGF-I-Mediated Growth

To determine whether the selective effects of NVP-ADW742 on IGF-I-mediated signaling translated into selective growth inhibition, H526 cells were incubated in serum-free medium with saturating concentrations of either IGF-I or SCF and increasing concentrations of the compound for 72 h. MTT assays demonstrated that IGF-I-mediated growth was inhibited by NVP-ADW742 with an IC_{50} of 0.2–0.4 μM, which correlated well with the inhibition of IGF-IR autophosphorylation. SCF-mediated growth was inhibited with an ~10-fold higher IC_{50} value, again correlating well with the ability of NVP-ADW742 to selectively inhibit IGF-IR signaling relative to Kit signaling (Fig. 3A).

To confirm the specificity of NVP-ADW742 toward the IGF-IR and determine the susceptibility of nontransformed cells to the drug, we also compared the ability of NVP-ADW742 to inhibit growth of R-cells, mouse embryonic fibroblasts derived from *IGF-IR−/−* embryos using a 3T3 protocol (5, 6), with NIH3T3 cells. Growth in serum-containing medium was assessed by MTT assay (Fig. 3B). Both murine fibroblast cell lines were resistant to the drug up to and including a concentration of 1 μM. At higher concentrations, wild-type 3T3 cells were markedly more sensitive to the effects of NVP-ADW742 (IC_{50} of 3 μM) than R-cells (IC_{50} of 9 μM), indicating that the drug selectively inhibits growth of cells expressing the IGF-IR.

NVP-ADW742 Inhibits Serum-Stimulated Growth of SCLC Cell Lines

To investigate the effect of NVP-ADW742 on growth in a complex mix of growth factors that tumors may encounter *in vivo*, MTT assays were performed in serum-containing medium using several representative SCLC cell lines (H526, H146, H209, and WBA) and a nontransformed human diploid pulmonary fibroblast cell line (MRC-5). All cell lines showed a dose-dependent inhibitory response but with a range of IC_{50} values (Fig. 4A). The assay results suggested two populations of SCLC cell lines as determined by drug sensitivity. One population represented by H526 and H146, which lack active SCF/Kit autocrine loops based on low or absent expression of SCF and Kit, respectively (27), was inhibited with IC_{50} values between 0.1 and 0.5 μM. A second population represented by WBA and H209, which coexpress both SCF and Kit (27), was inhibited with a higher IC_{50} value of 4–7 μM. Growth of MRC-5 was moderately inhibited, but no cell death occurred even at 10 μM NVP-ADW742. Normal human bronchial epithelial cells showed an IC_{50} of 4.2 μM (data not shown), approximating the sensitivity of the more resistant SCLC cell lines. However, their enhanced sensitivity to NVP-ADW742 relative to MRC-5 may be due to their derivation and continuous propagation in serum-free medium containing high insulin concentrations (capable of activating the IGF-IR), which could select for cells more dependent on IGF-IR signaling.

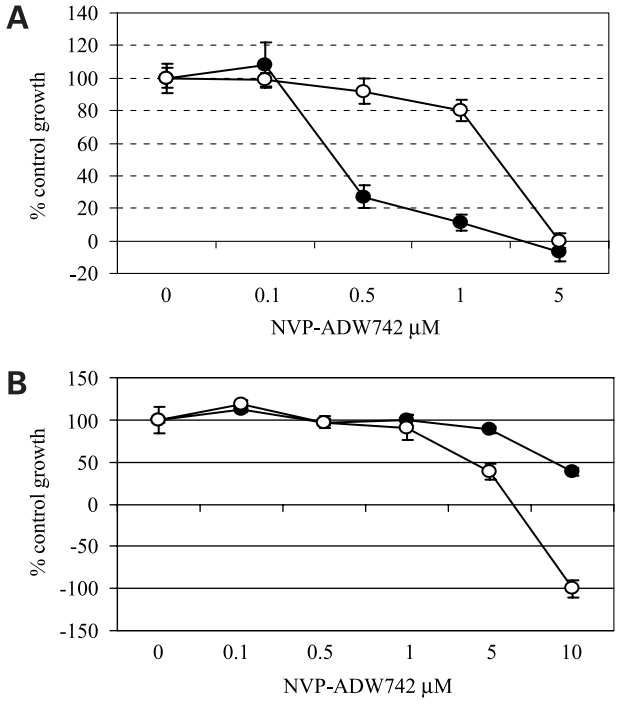

Figure 3. NVP-ADW742 selectively inhibits IGF-I-mediated growth. **A,** H526 cells were incubated in serum-free medium in the presence of either IGF-I (●) or SCF (○) and increasing concentrations of NVP-ADW742. Growth was assessed by the MTT dye reduction assay after 72 h. **B,** MTT assays with R- (●) and 3T3 (○) cells in the presence of 10% FBS and increasing concentrations of NVP-ADW742. Representative of at least three individual experiments. *Points,* mean of eight replicate wells; *bars,* SE.

SCF Protects H526 Cells from Growth Inhibition by NVP-ADW742

We hypothesized that H526 and H146 were very sensitive to IGF-IR inhibition by NVP-ADW742 because they lack a functional SCF/Kit autocrine loop. One way of testing this hypothesis would be to add recombinant SCF to complete medium and determine whether the sensitivity of H526 to NVP-ADW742 is altered, because this cell line expresses Kit but lacks significant SCF production (and 10% FBS contains little SCF). Figure 4B clearly demonstrates that SCF protects H526 from growth inhibition at NVP-ADW742 concentrations between 0.5 and 5 μM. This protection is particularly evident at 1 μM, a concentration that inhibits virtually all IGF-IR-mediated signal transduction but has relatively little effect on Kit-mediated signaling (Figs. 1, 2A, and 3A). This protection is largely lost at NVP-ADW742 concentrations

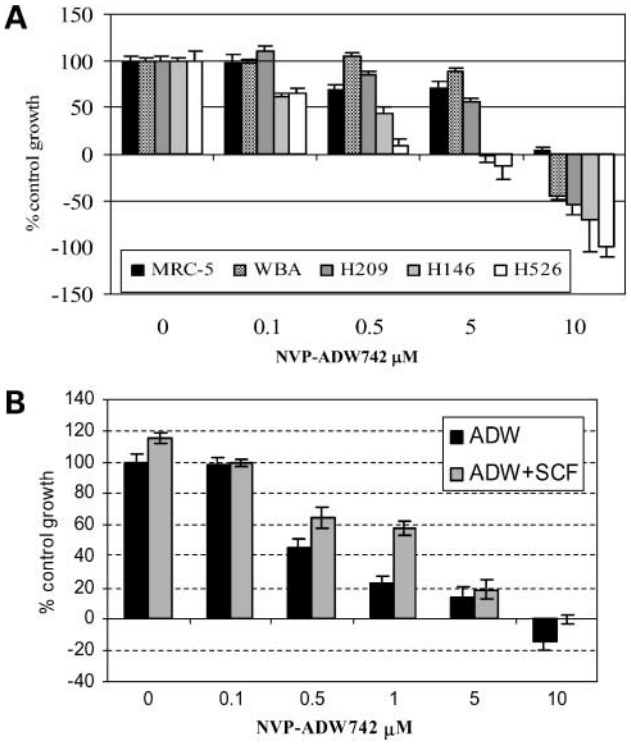

Figure 4. Kit activation modulates sensitivity of SCLC cells to NVP-ADW742. **A,** MTT assays were performed with SCLC cell lines H526, H146, H209, WBA and a fibroblast cell line MRC-5 in the presence of 10% FBS and increasing concentrations of NVP-ADW742. H209 and WBA coexpress SCF and Kit, whereas H526 and H146 do not. **B,** an MTT growth assay to determine NVP-ADW742 dose response was performed with H526 cells in the presence or absence of 100 ng/ml SCF in medium containing 10% FBS. SCF clearly protects H526 at NVP-ADW742 concentrations between the IC_{50} values for IGF-IR and Kit, respectively. Representative of at least three individual experiments. *Columns,* mean of eight replicate wells; *bars,* SE.

≥ 5 μM, which effectively inhibit Kit signaling (Figs. 2A and 3A). Thus, these data support the concept that for optimum growth inhibition of SCLC, it is necessary to inhibit both IGF-IR and Kit signaling.

Combination of NVP-ADW742 and STI571 Treatment Is Synergistic

Based on the above findings, one possible explanation for the resistance of WBA and H209 would be that in these cell lines, NVP-ADW742 must inhibit not only IGF-IR but also Kit, which requires a higher drug concentration. STI571 affects SCLC growth through inhibition of Kit signaling (22). To obtain further documentation as to whether inhibition of both IGF-I and SCF signaling is required for optimal growth inhibition of SCLC, we studied the response to treatment with a combination of NVP-ADW742 and STI571. When the dose-effect relationship for the combination was determined using the four representative SCLC cell lines, no advantage over NVP-ADW742 alone was seen with H526 and H146 cells (data not shown), but a clear synergistic response was seen with the WBA (Fig. 5A) and H209 (data not shown) cell lines. Growth data obtained in MTT assays were used in calculation of the combination index according to the Chou and Talalay multiple drug effect equation (29) to measure the degree of synergism, where a combination index value of <1 indicates synergism. This analysis revealed a value of 0.27 for WBA (strong synergism) and 0.43 for H209 at a fraction affected of 50%.

To determine whether the combination of NVP-ADW742 and STI571 had an additive or synergistic effect on proliferative signal transduction, the effect of the drug combination on Akt activation was studied in WBA cells under serum and serum-free conditions. NVP-ADW742 alone had no effect on Akt activation in serum and only a modest effect on the high basal activity in this cell line in serum-free medium (Fig. 5B). However, the addition of 5 or 10 μM STI571 to NVP-ADW742 restored a robust dose-dependent reduction in Akt activation. This appeared to be a synergistic interaction. For example, in serum, 10 μM NVP-ADW742 had no effect on Akt activity. However, addition of 5 μM STI571, which also had minimal effect on Akt activity by itself (94% of control),

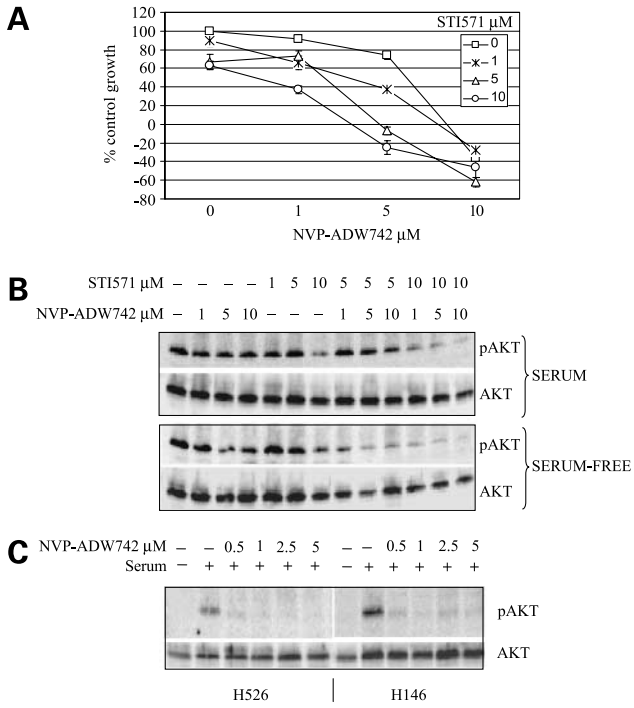

Figure 5. Combination treatment with NVP-ADW742 and STI571 synergistically inhibits growth and PI3K-Akt signaling. **A,** an MTT growth assay was carried out with WBA cells in complete medium treated with either STI571 or NVP-ADW742 or a combination of the two drugs for 72 h. A clear STI571 dose-dependent decrease in growth was observed with the combination treatment. *Points,* mean of eight replicate wells; *bars,* SE. **B,** Western analysis was performed using whole cell lysates to monitor Akt activity [pAkt (Ser^{473})] in WBA cells treated with a combination of NVP-ADW742 and STI571 for 1 h in complete or serum-free medium. **C,** Western analysis was performed using whole cell lysates to monitor Akt activity [pAkt (Ser^{473})] in H526 and H146 cells pretreated with NVP-ADW742 for 1 h and incubated in complete medium for 6 h.

clearly resulted in a marked reduction in Akt activity (55% of control). Thus, the effect of the drug combination on the critical PI3K-Akt signal transduction pathway correlated well with its synergistic effect on growth.

The results depicted in Fig. 5B suggest that efficient inhibition of PI3K-Akt signaling is a prerequisite for growth inhibition and that, in the resistant WBA cell line, this requires inhibition of both IGF-IR and Kit. It follows then that in cell lines sensitive to NVP-ADW742, the drug should efficiently inhibit PI3K-Akt signaling as a single agent. To test this prediction, we exposed the H526 and H146 cell lines to increasing concentrations of NVP-ADW742 in complete medium and assessed the level of Akt activation. Figure 5C illustrates that NVP-ADW742 efficiently inhibited Akt activation induced by serum components in complete medium and did so at concentrations consistent with the IC_{50} of IGF-IR. These data provide further evidence that cell lines that are sensitive to NVP-ADW742 are highly dependent on IGF-I in serum for activation of critical signaling pathways.

The MTT assay in Fig. 5A illustrates that the combination of NVP-ADW742 and STI571 was cytotoxic to WBA cells when 5 or 10 μM concentrations of each drug were used. To document that the cytotoxicity observed was due to apoptosis, a TdT-mediated nick end labeling assay was performed following a 24 h incubation in increasing concentrations of NVP-ADW742 alone or in combination with 5 μM STI571 (Fig. 6). STI571 alone or NVP-ADW742 alone up to and including a concentration of 5 μM did not increase the degree of apoptosis above control. However, combination of 1 or 5 μM NVP-ADW742 with STI571 resulted in nearly a doubling of the degree of apoptosis relative to control or NVP-ADW742-treated cultures. This synergism was largely lost at 10 μM NVP-ADW742, a concentration that produces significant inhibition of Kit. It is noteworthy that the combination of 5 μM NVP-ADW742 and STI571 resulted in a degree of apoptosis approaching that induced by 25 μM etoposide, a high concentration of one of the most active single chemotherapeutic agents used in the treatment of SCLC.

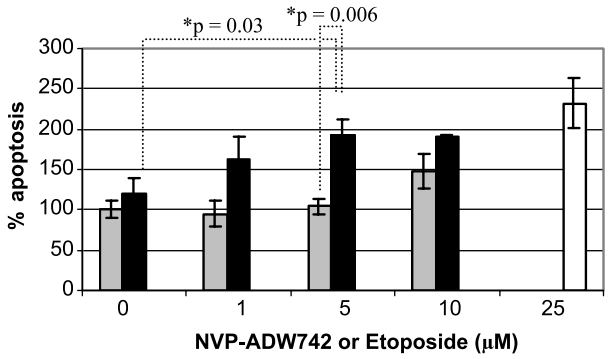

Figure 6. Combination treatment with NVP-ADW742 and STI571 synergistically induces apoptosis. WBA cells treated for 24 h in complete medium with NVP-ADW742 alone (*gray bars*) or in combination with 5 μM STI571 (*black bars*) were assessed for apoptosis by TdT-mediated nick end labeling assay. Data are expressed as percentage of apoptosis relative to the vehicle control (0 μM NVP-ADW742), which was arbitrarily assigned a value of 100%. Apoptosis was significantly higher in cells treated with 5 μM NVP-ADW742 + 5 μM STI571 compared with 5 μM NVP-ADW742 alone ($P = 0.006$) or 5 μM STI571 alone ($P = 0.03$). There was no statistical difference in apoptosis between the vehicle control and cells treated with STI571 alone (0 μM NVP-ADW742 + STI571). There was also no statistically significant difference between cells treated with STI571 + 10 μM NVP-ADW742 and 10 μM NVP-ADW742 alone. Cells were treated with 25 μM etoposide (*white bar*) as a positive control. Representative of three individual experiments. *Columns,* mean; *bars,* SE.

Discussion

IGF-I signaling has become an attractive target for novel cancer therapeutics based on its role in promoting tumor growth and survival (11, 14, 30). The development of potent and selective agents that can interrupt IGF-I signaling has been challenging, however (30). Several investigators have reported inhibition of IGF-I signaling in tumors using a variety of approaches. For the treatment of malignant astrocytomas, *ex vivo* IGF-IR antisense oligonucleotide treatment of autologous glioma cells was shown to induce apoptosis and a host response *in vivo* in a pilot study (31). Other approaches include blocking the ligand-receptor interaction using competitive inhibitors (32, 33), use of stable antisense IGF-IR RNA to inhibit tumor cell growth (34), and use of antibodies against IGF-IR (35). Gene therapy approaches using adenoviruses expressing dominant-negative IGF-IR have also proven to be effective against established lung cancer xenografts (36). Targeting of other tyrosine kinases with potent and selective small molecule inhibitors has been a very useful strategy (37), but the major difficulty in using such an approach for targeting the IGF-IR has been the need for agents that exhibit selectivity for IGF-IR *versus* the insulin receptor. Despite the high degree of homology between these two receptors, preliminary studies suggested that it would be possible to design selective small molecule IGF-IR inhibitors (32). We were particularly interested in the development of an IGF-IR inhibitor because of the observation that IGF-I is an efficient antagonist of SCLC apoptosis mediated by STI571, a potent inhibitor of the Kit receptor tyrosine kinase (22). In the present study, we have shown that a novel pyrrolo[2,3-*d*]pyrimidine compound, NVP-ADW742, selectively inhibits IGF-I-mediated growth and signal transduction in SCLC cells and synergizes with the growth inhibitory effects of STI571.

NVP-ADW742 has an ~15-fold selectivity for the IGF-IR (IC_{50} of 0.17 μM) *versus* the insulin receptor (IC_{50} of 2.8 μM) in model cellular autophosphorylation assays using NIH3T3 cells transfected with the corresponding human receptors (24, 25). The mean IC_{50} of 0.1 μM for inhibition of IGF-IR autophosphorylation in H526 cells (Fig. 1) is consistent with those results. The observation that the IC_{50} for Kit is in the 2–5 μM range in SCLC (Fig. 2A) is interesting, because while it does illustrate that NVP-ADW742 has selectivity for IGF-IR, it also demonstrates that the drug has the potential to inhibit two receptors relevant to SCLC growth. The differential in the IC_{50} values for inhibition of IGF-IR and Kit phosphorylation was

maintained when IGF-I- and SCF-mediated growth was assessed (Fig. 3A), illustrating that selectivity for the IGF-IR was maintained in a functional assay. Selectivity of the drug was further documented by demonstrating a lack of direct effects on Met- and Akt-mediated signal transduction and the relative resistance of fibroblasts lacking IGF-IR to growth inhibition (Fig. 3B).

While targeting receptor tyrosine kinase signaling is a promising anticancer strategy, a major roadblock that could be anticipated when highly selective kinase inhibitors are used is that, in most tumors, multiple receptor tyrosine kinases are expressed and each is capable of activating an overlapping spectrum of critical downstream signaling pathways. For example, both SCF and IGF-I are potent growth factors for SCLC and are capable of activating the PI3K-Akt pathway, which is the predominant growth stimulatory pathway for SCLC (20). Expression of a constitutively active myristolated *Akt* allele alone was sufficient to drive H526 growth, approximating levels attained in the presence of either IGF-I or 10% FBS. Given this observation, it is not surprising that inhibition of Kit signaling with STI571, in the presence of serum containing IGF-I, produced only modest growth inhibition of a panel of SCLC cell lines (22). It is also not surprising then that in the present study, SCLC cell lines showed a range of sensitivity to potent inhibition of IGF-IR with NVP-ADW742. The H526 and H146 cell lines, which lack functional SCF/Kit autocrine loops, were highly sensitive to the drug (Fig. 4A) with antiproliferative IC_{50} values approximating those for inhibition of IGF-IR autophosphorylation. On the other hand, the H209 and WBA cell lines, which have functional SCF/Kit autocrine loops, were less sensitive with IC_{50} values nearly 10-fold higher, approximating the IC_{50} values obtained for Kit kinase inhibition. This latter observation suggested that in these cell lines, growth inhibition required inhibition of both IGF-IR and Kit signaling. In support of this hypothesis, we demonstrated that activation of Kit in H526 cells by addition of SCF resulted in protection from growth inhibition at NVP-ADW742 concentrations between the IC_{50} values for IGF-IR and Kit, respectively (Fig. 4B). To obtain additional evidence supporting this hypothesis, we also demonstrated that treatment of the WBA and H209 cell lines with a combination of NVP-ADW742 and STI571 produced synergistic growth inhibition as well as induction of apoptosis (Figs. 5A and 6). Most importantly, growth suppression by these kinase inhibitors correlated very well with inhibition of Akt activation, a marker of the pathway largely responsible for SCLC growth and protection from apoptosis (Fig. 5, B and C). In fact, the strong correlation between growth suppression and inhibition of Akt activation suggests that assessment of the relative change in Akt activity could serve as a useful biomarker in this disease, especially when assessing the efficacy of combinations of upstream kinase inhibitors.

Multiple potential strategies exist for the therapeutic inhibition of oncogenic signal transduction. Receptors can be targeted with small molecules and specific biologics such as monoclonal antibodies or soluble receptor analogs. Downstream signal transduction can be targeted with a variety of small molecule approaches, either at proximal nodes of convergence from multiple receptors, at distal transcription factors, or at multiple intermediary levels. The best current model for success is the treatment of chronic myelogenous leukemia and gastrointestinal stromal tumors with the tyrosine kinase inhibitor STI571, which targets signal transduction from Bcr-Abl and mutationally activated Kit, respectively (38). However, few tumor types, especially epithelial malignancies, will be driven by a single oncogenic kinase; therefore, treatment of these malignancies will require more complex strategies. Biological studies will have to provide solid evidence for the relevance of specific receptors and downstream signaling pathways and these pathways will need to be targeted using the most efficient and selective strategies. In SCLC, we have illustrated that inhibition of PI3K-Akt signaling using a combination of IGF-IR and Kit inhibitors is an effective strategy for inhibiting growth *in vitro*. It remains to be seen whether the class of small molecule IGF-IR inhibitors described here will have an acceptable therapeutic index on further *in vivo* testing. The availability of selective IGF-IR inhibitors could not only be a major advance in the treatment of SCLC but also a wide range of epithelial malignancies where IGF-I has been shown to play an important role regulating growth, apoptosis, and angiogenesis. However, for the broadest applicability and the best efficacy, IGF-IR inhibitors will likely have to be used in combination with strategies to inhibit signaling from other relevant receptors.

References

1. Stiles AD, D'Ercole AJ. The insulin-like growth factors and the lung. Am J Respir Cell Mol Biol 1990;3:93 – 100.
2. D'Ercole AJ. Insulin-like growth factors and their receptors in growth. Endocrinol Metab Clin North Am 1996;25:573 – 90.
3. Sell C, Rubini M, Rubin R, Liu JP, Efstratiadis A, Baserga R. Simian virus 40 large tumor antigen is unable to transform mouse embryonic fibroblasts lacking type 1 insulin-like growth factor receptor. Proc Natl Acad Sci USA 1993;90:11217 – 21.
4. Sell C, Dumenil G, Deveaud C, et al. Effect of a null mutation of the insulin-like growth factor I receptor gene on growth and transformation of mouse embryo fibroblasts. Mol Cell Biol 1994;14:3604 – 12.
5. Liu JP, Baker J, Perkins AS, Robertson EJ, Efstratiadis A. Mice carrying null mutations of the genes encoding insulin-like growth factor I (Igf-1) and type 1 IGF receptor (Igf1r). Cell 1993;75:59 – 72.
6. Baker J, Liu JP, Robertson EJ, Efstratiadis A. Role of insulin-like growth factors in embryonic and postnatal growth. Cell 1993;75:73 – 82.
7. Furlanetto RW, Harwell SE, Frick KK. Insulin-like growth factor-I induces cyclin-D1 expression in MG63 human osteosarcoma cells *in vitro.* Mol Endocrinol 1994;8:510 – 7.
8. Kulik G, Klippel A, Weber MJ. Antiapoptotic signaling by the insulin-like growth factor I receptor, phosphatidylinositol 3-kinase, and Akt. Mol Cell Biol 1997;17:1595 – 606.
9. Minshall C, Arkins S, Straza J, et al. IL-4 and insulin-like growth factor-I inhibit the decline in Bcl-2 and promote the survival of IL-3-deprived myeloid progenitors. J Immunol 1997;159:1225 – 32.
10. Parrizas M, LeRoith D. Insulin-like growth factor-1 inhibition of apoptosis is associated with increased expression of the bcl-xL gene product. Endocrinology 1997;138:1355 – 8.
11. Valentinis B, Baserga R. IGF-I receptor signaling in transformation and differentiation. Mol Pathol 2001;54:133 – 7.
12. LeRoith D, Baserga R, Helman L, Roberts CT Jr. Insulin-like growth factors and cancer. Ann Intern Med 1995;122:54 – 9.

13. Furstenberger G, Senn HJ. Insulin-like growth factors and cancer. Lancet Oncol 2002;3:298 – 302.

14. Yu H, Rohan T. Role of the insulin-like growth factor family in cancer development and progression. J Natl Cancer Inst 2000;92:1472 – 89.

15. Yu H, Spitz MR, Mistry J, Gu J, Hong WK, Wu X. Plasma levels of insulin-like growth factor-I and lung cancer risk: a case-control analysis. J Natl Cancer Inst 1999;91:151 – 6.

16. Ihde D, Pass H, Glatstein E. Small cell lung cancer. In: DeVita V, Hellman S, Rosenberg S, editors. Cancer: principles and practice of oncology. Philadelphia: Lippincott; 1997. p. 911 – 49.

17. Macaulay VM. Insulin-like growth factors and cancer. Br J Cancer 1992;65:311 – 20.

18. Jaques G, Kiefer P, Rotsch M, et al. Production of insulin-like growth factor binding proteins by small-cell lung cancer cell lines. Exp Cell Res 1989;184:396 – 406.

19. Nakanishi Y, Mulshine JL, Kasprzyk PG, et al. Insulin-like growth factor-I can mediate autocrine proliferation of human small cell lung cancer cell lines *in vitro.* J Clin Invest 1988;82:354 – 9.

20. Krystal G, Sulanke G, Litz J. Inhibition of phosphatidylinositol 3-kinase-Akt signaling blocks growth, promotes apoptosis and enhances sensitivity of small cell lung cancer cells to chemotherapy. Mol Cancer Ther 2002;1:913 – 22.

21. Buchdunger E, Cioffi CL, Law N, et al. Abl protein-tyrosine kinase inhibitor STI571 inhibits *in vitro* signal transduction mediated by c-kit and platelet-derived growth factor receptors. J Pharmacol Exp Ther 2000; 295:139 – 45.

22. Krystal GW, Honsawek S, Litz J, Buchdunger E. The selective tyrosine kinase inhibitor STI571 inhibits small cell lung cancer growth. Clin Cancer Res 2000;6:3319 – 26.

23. Wang WL, Healy ME, Sattler M, et al. Growth inhibition and modulation of kinase pathways of small cell lung cancer cell lines by the novel tyrosine kinase inhibitor STI 571. Oncogene 2000;19:3521 – 8.

24. García-Echeverría C, Brueggen J, Capraro H-G, et al. Characterization of potent and selective kinase inhibitors of IGF-1R. Proc Am Assoc Cancer Res 2003;44(2nd ed):203.

25. Mitsiades CS, Mitsiades N, Kung AL, et al. The IGF/IGF-1R system is a major therapeutic target for multiple myeloma, other hematologic malignancies and solid tumors. Cancer Cell 2004;5:221 – 30.

26. Carney DN, Gazdar AF, Bepler G, et al. Establishment and identification of small cell lung cancer cell lines having classic and variant features. Cancer Res 1985;45:2913 – 23.

27. Plummer H III, Catlett J, Leftwich J, et al. c-*myc* expression correlates with suppression of c-kit protooncogene expression in small cell lung cancer cell lines. Cancer Res 1993;53:4337 – 42.

28. Carmichael J, DeGraf WG, Gazdar AD, Minna JD, Mitchell JB. Evaluation of a tetrazolium-based semiautomated colorimetric assay: assessment of chemosensitivity testing. Cancer Res 1987;47:936 – 42.

29. Chou TC, Talalay P. Applications of the median-effect principle for the assessment of low-dose risk of carcinogens and for the quantitation of synergism and antagonism of chemotherapeutic agents. In: Bristol-Myers Symposium Series; 1987. p. 37 – 64.

30. Yee D. Are the insulin-like growth factors relevant to cancer? Growth Horm IGF Res 2001;11:339 – 45.

31. Andrews DW, Resnicoff M, Flanders AE, et al. Results of a pilot study involving the use of an antisense oligodeoxynucleotide directed against the insulin-like growth factor type I receptor in malignant astrocytomas. J Clin Oncol 2001;19:2189 – 200.

32. Blum G, Gazit A, Levitzki A. Substrate competitive inhibitors of IGF-1 receptor kinase. Biochemistry 2000;39:15705 – 12.

33. Pietrzkowski Z, Mulholland G, Gomella L, Jameson BA, Wernicke D, Baserga R. Inhibition of growth of prostatic cancer cell lines by peptide analogues of insulin-like growth factor 1. Cancer Res 1993; 53:1102 – 6.

34. Neuenschwander S, Roberts CT Jr, LeRoith D. Growth inhibition of MCF-7 breast cancer cells by stable expression of an insulin-like growth factor I receptor antisense ribonucleic acid. Endocrinology 1995;136: 4298 – 303.

35. Li SL, Liang SJ, Guo N, Wu AM, Fujita-Yamaguchi Y. Single-chain antibodies against human insulin-like growth factor I receptor: expression, purification, and effect on tumor growth. Cancer Immunol Immunother 2000;49:243 – 52.

36. Lee CT, Park KH, Adachi Y, et al. Recombinant adenoviruses expressing dominant negative insulin-like growth factor-I receptor demonstrate antitumor effects on lung cancer. Cancer Gene Ther 2003;10: 57 – 63.

37. Shawver LK, Slamon D, Ullrich A. Smart drugs: tyrosine kinase inhibitors in cancer therapy. Cancer Cell 2002;1:117 – 23.

38. Mauro MJ, O'Dwyer M, Heinrich MC, Druker BJ. STI571: a paradigm of new agents for cancer therapeutics. J Clin Oncol 2002;20:325 – 34.